Original Article

Institution of MECHANICAL ENGINEERS
Journal of AUTOMOBILE ENGINEERING

Proc IMechE Part D:
J Automobile Engineering
1–14

DOI: 10.1177/0954407015581082
pid.sagepub.com
SAGE

Cooperative control of regenerative braking and friction braking for a hybrid electric vehicle

CS Nanda Kumar and Shankar C Subramanian

Abstract

In this paper, a rear-wheel-driven series hybrid electric vehicle which has a mechanically operated friction brake system is studied. A new cooperative control of regenerative braking and friction braking called 'combined braking' is proposed for this vehicle configuration. A mechanism to adjust the proportions of regenerative braking and friction braking was proposed in this paper. Further, the braking force distribution between the front wheels and the rear wheels was analysed to ensure stable braking. The brake system characteristics were considered to ensure that the driver's feel remains the same in the new proposed combined braking strategy. The simulation results under urban driving and across the Modified Indian Driving Cycle and vehicle road testing results show that the proposed combined braking can regenerate more than twice the braking energy of conventional parallel braking. Also, with combined braking, the braking force distribution between the front wheels and the rear wheels is closer to the ideal braking force distribution curve, which is desirable to ensure stable braking.

Keywords

Hybrid electric vehicle, regenerative braking, braking force distribution

Date received: 2 April 2014; accepted: 3 March 2015

Introduction

Regenerative braking is a key technology that improves the overall efficiency in electric vehicles (EVs) and hybrid electric vehicles (HEVs). During regenerative braking, the kinetic and potential energies of the vehicle are converted into electrical energy and stored in a battery or a supercapacitor for driving. Regenerative braking is more effective in city driving conditions, where the brakes are applied more frequently. Regenerative braking can improve the fuel efficiency of the vehicle from 20% to 50%, depending on the motor size.[1] According to Li et al.,[2] about one third to one half of the energy is consumed in braking in urban driving, which can be potentially recuperated. Toyota has reported that, with regenerative braking, the overall fuel efficiency has improved by 35% in a series– parallel configuration HEV.[3]

In most cases, the regenerative brake works together with the conventional friction brake to meet the total braking force demand. Under some conditions such as a high state of charge (SOC) of the battery or low-speed braking, the regenerative brake is limited and only the friction brake is applied. Hence, cooperative control of the regenerative brake and the friction brake is always required to generate an adequate braking force.[4,5] Honda has reported that the parallel hybrid test vehicle has regenerated 46% more energy with cooperative control than with non-cooperative control.[6]

The regenerative braking configuration can be broadly classified into series braking and parallel braking.[7,8] In series braking, cooperative control of the friction brake and the regenerative brake is achieved by the vehicle controller together with the motor controller and the friction brake controller. In series braking, the regenerative brake is mostly applied first before the friction brake. As explained by Zhang et al.,[9] it is possible to achieve either maximum energy regeneration or good pedal feel at all conditions in series braking.

Department of Engineering Design, Indian Institute of Technology Madras, Chennai, India

Corresponding author:
Shankar C Subramanian, Department of Engineering Design, Indian Institute of Technology Madras, Chennai 600036, India.
Email: shankarram@iitm.ac.in

The parallel regenerative braking system is relatively simple; the energy recovered by the regenerative braking system will be small, and the driveability of the vehicle may be affected.[10] In conventional parallel braking, both the friction brake and the regenerative brake are applied in parallel, and no cooperative control takes place between the friction brake and the regenerative brake. As explained by Ehsani et al.,[14] the vehicle controller controls only the regenerative braking torque, whereas the friction braking torque is controlled directly by the brake pedal displacement in parallel braking. This type of configuration is used in EVs or HEVs which have a mechanically controlled friction brake.

Recent research has focused on various regenerative braking control strategies and their benefits for EVs and HEVs which have a series braking configuration.[5,7] Since EVs and HEVs in emerging markets such as India have a mechanically controlled friction brake, where the series braking configuration cannot be adapted because of its high cost, parallel braking is a feasible solution. However, conventional parallel braking has a low energy regeneration capability. Hence, improving the energy regeneration in conventional parallel braking is the key focus of this paper. A simple cooperative solution called 'combined braking' is proposed, which can double the energy regeneration in comparison with that of conventional parallel braking in EVs or HEVs which have a mechanically controlled friction brake. This new concept is an improvement over conventional parallel braking with minimum modifications to the existing brake system, which makes it cost effective. In combined braking, the braking power of the electric motor is used to its full potential before the friction brakes are applied.

Further, the braking force is applied only on the driven wheels in regenerative braking. The non-driven wheels are not subjected to braking during the regenerative braking mode. For stable braking of any vehicle, the braking force distribution (BFD) between the front wheels and the rear wheels should balance the dynamic limit of the vehicle.[11] Therefore, apart from the energy regeneration perspective, a detailed analysis was also made of the BFD with both the parallel braking configuration and the combined braking configuration.

Another challenge in regenerative braking is the driver's feel. In EVs and HEVs, the total braking force generated can be in three modes: the friction brake mode, the regenerative brake mode and a combination of the two. In all modes, the driver should have the same feel (in terms of the vehicle deceleration) for a given brake pedal displacement. In order to evaluate this issue, the friction brake system characteristics of the experimental vehicle were obtained and used in the design and analysis.

A series hybrid electric vehicle (SHEV) is one of the powertrain configurations of HEVs, in which the electric motor is the prime mover that drives the wheels, as shown in Figure 1. The engine coupled with a generator charges the battery and also supplies electric power directly to the motor. In this configuration, the power rating of the motor should be sufficiently high to meet the drive performance of the vehicle such as the acceleration, the maximum speed and the gradeability. In an SHEV with a higher motor power rating, regenerative braking is mostly used to the maximum extent prior to the introduction of friction braking.[11]

Since an SHEV has a higher motor power, it has the potential to regenerate more, and it can influence the BFD to a higher extent. Hence, this configuration was

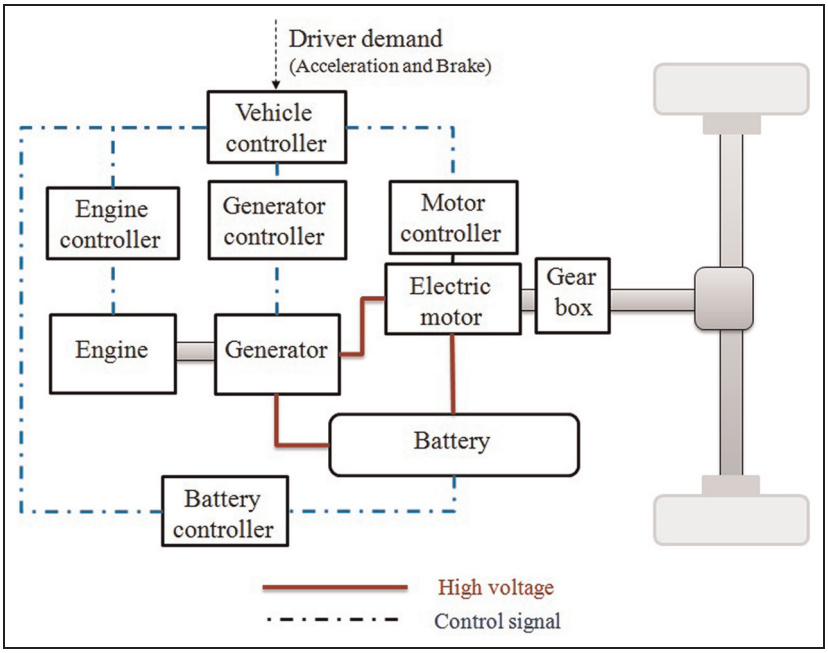

Figure 1. System layout of an SHEV.

considered in this paper for analysing the energy regeneration and the BFD between the front wheels and the rear wheels for both combined braking and conventional parallel braking. Simulations and road tests were carried out, and the results were compared and discussed for both configurations.

The remainder of this paper is organized as follows. In the second section the friction brake system characteristics are considered, and in the third section the combined regenerative braking and conventional parallel braking concepts are discussed. The longitudinal dynamics of the vehicle and the limiting curves for the braking force are explained in the fourth section. The simulation results and the road test results are presented in the fifth section and the sixth section respectively, and conclusions are drawn in the seventh section.

Friction brake system characteristics

In this study, the characteristics of the friction brake system were derived by obtaining the relationship between the braking force generated and the corresponding brake pedal displacement. This has been considered to incorporate the driver's feel, since a braking force results in a corresponding vehicle deceleration that is felt by the driver. Hence, the braking force (which results in a corresponding deceleration) was considered as a measure to quantify the driver's feel. This characteristic of the friction brake was obtained experimentally and then used to ensure that, for a given brake pedal displacement, the combined braking strategy provides the same level of brake feel (in other words, the same amount of vehicle deceleration) as that of a standalone friction brake system. This characteristic, together with the objective of regenerating the maximum possible energy, was used to decide the proportions of regenerative braking and friction braking in the combined braking strategy.

The experimental vehicle (the parameters of which are given in Table 1) was used to estimate the friction brake system characteristics.

The brake pedal displacement L_p was measured using a linear displacement sensor. The motor controller receives the signal of the motor speed N (r/min), and the longitudinal speed V (m/s) of the vehicle was inferred from it using

$$V = \frac{1 - S}{\mathrm{TR}} \frac{2\pi N}{60} r \tag{1}$$

where r is the effective tyre radius (m), TR is the transmission ratio and S is the percentage of longitudinal slip between the tyres and the road. This equation was used to evaluate the longitudinal speed of the experimental vehicle. Also, this equation could be used to calculate reasonably the vehicle velocity under 'normal' operating conditions (i.e. excluding events such as excessive wheel slip leading to wheel lock). Since the objective of this study was to evaluate the performance of the proposed combined braking strategy under such conditions, the above equation was used to calculate the longitudinal speed of the vehicle. The test vehicle was braked from an initial speed of V_i and the time taken for it to stop was recorded. Using this, the average deceleration a was obtained and the braking force was calculated using

$$F_b = Ma - Mgf_r - \tfrac{1}{2}\rho_a C_d A_f V^2 \tag{2}$$

where M is the mass of the vehicle (kg), g is the acceleration due to gravity (m/s^2), f_r is the rolling resistance coefficient, ρ_a is the density of air (kg/m^3), C_d is the coefficient of aerodynamic drag, A_f is the frontal area of the vehicle (m^2) and V is the average velocity of the vehicle (m/s). This experimental process was repeated for various brake pedal displacements in steps of 5 mm, up to a maximum displacement of 40 mm. The corresponding data are plotted in Figure 2.

Table 1. Experimental vehicle parameters.

Mass M	1800 kg
Frontal area A_f	2.93 m^2
Drag coefficient C_d	0.4
Rolling resistance coefficient f_r	0.02
Continuous power P_m of the motor	11 kW
Base speed N_1 of the motor	1600 r/min
Maximum speed N_2 of the motor	6000 r/min
Operating voltage U	96 V
Capacity E of the lead–acid battery	24 kW h
Brake pedal ratio PR	6
Transmission ratio TR	13.39
Radius r of the wheels	0.25 m
Wheelbase L	1.84 m
Distance L_a from the front axle to the centre of gravity	1.23 m
Distance L_b from the rear axle to the centre of gravity	0.61 m
Height h of the centre of gravity from the ground	0.6 m
Tyre slip S	0.1

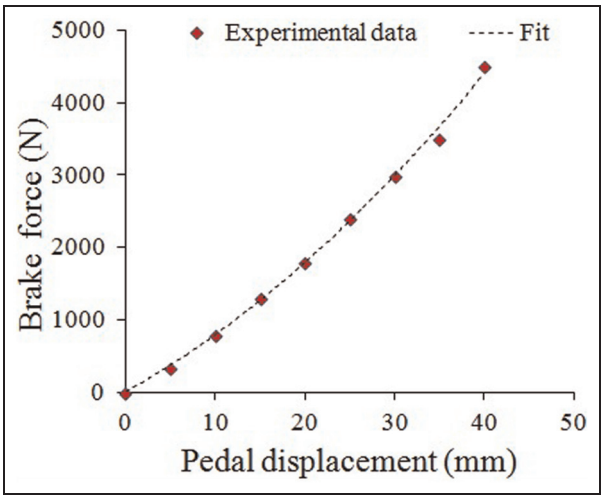

Figure 2. Characteristics of the friction brake system.

Table 2. Constants of the brake system characteristics.

A_0	1.03×10^6 N/m^2
A_1	68.9×10^3 N/m
A_2	3.3 N
B_0	-8×10^{-10} m/N^2
B_1	0.012×10^{-3} m/N
B_2	0.382×10^{-3} m

These data points were fitted to obtain the relationship

$$F_b = A_0 L_p^2 + A_1 L_p + A_2 \quad (3)$$

Equation (3) represents the characteristics of the friction brake system of the vehicle considered. The corresponding inverse relationship is

$$L_p = B_0 F_b^2 + B_1 F_b + B_2 \quad (4)$$

The values of the parameters A_0, A_1, A_2, B_0, B_1 and B_2 are given in Table 2.

Equations (3) and (4) were used in designing the combined braking strategy and also for ensuring the same driver's feel, while blending the friction brake and the regenerative brake.

Regenerative braking

As discussed in the introduction, the regenerative braking configuration is broadly classified into series braking and parallel braking. Since the objective of this study is to improve the energy regeneration in EVs and HEVs which have a mechanically controlled friction brake system, parallel braking is considered as the base configuration in this paper. The proposed combined braking and conventional parallel braking concepts are elaborated in this section. The mathematical formulations are discussed in detail for both concepts.

Combined braking

The main objective of the proposed combined braking system is to regenerate the maximum energy in an EV or an HEV which is equipped with a mechanically controlled friction brake system. This objective was achieved with the proposed combined braking concept by the following two methods.

1. Only regenerative braking was applied and the activation of the friction brake for a predefined pedal displacement (OP in Figure 3) was isolated. The point P is determined from the braking power of the motor and the initial speed of the vehicle.
2. While braking is in process and when the vehicle speed starts to decrease, the friction braking force is reduced by varying the displacement of the master cylinder plunger and increasing the regenerative brake.

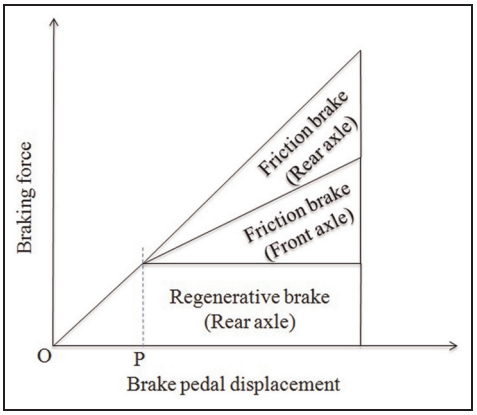

Figure 3. Sharing of the braking force in combined braking.

Detailed explanations of the combined braking system, the functionality and the mathematical modelling are given below.

System description. Figure 4(a) provides the schematic layout of the proposed combined braking concept which consists of standard components such as the brake pedal, the brake booster, the master cylinder and the pedal travel sensor. In addition, a linear solenoid actuator (LSA) was introduced between the brake pedal and the brake booster, and it is controlled by the vehicle controller. The LSA performs the following two basic functions.

1. It creates a predefined gap (OA in Figure 4(a)) between the brake pedal and the brake booster to delay the actuation of the friction brake in response to the driver's brake demand through the application of the brake pedal. The actuator displacement equivalent to the gap OA is termed the 'idle actuator displacement' and the pedal travel equivalent to OA is termed the 'idle pedal displacement' L_i.
2. While braking is in progress, it regulates the friction braking force by controlling the displacement (BC in Figure 4(a)) of the master cylinder plunger.

During normal driving conditions, the actuator is retracted such that it maintains the predefined gap OA between the actuator and the brake booster. During the actuator displacement equivalent to OA, the brake booster and the master cylinder are not actuated to apply the friction brake.

The displacement of the actuator beyond OA creates a mechanical contact between the actuator and the booster; because of this, the actuating force is transferred to the master cylinder to apply the friction brake. In the case of any failure in the signal or the supply current to the solenoid actuator, the compressed spring inside the actuator will return the actuator plunger to a fail-safe position, which will close the gap OA. This ensures that the conventional friction brake is available as a secondary or emergency option.

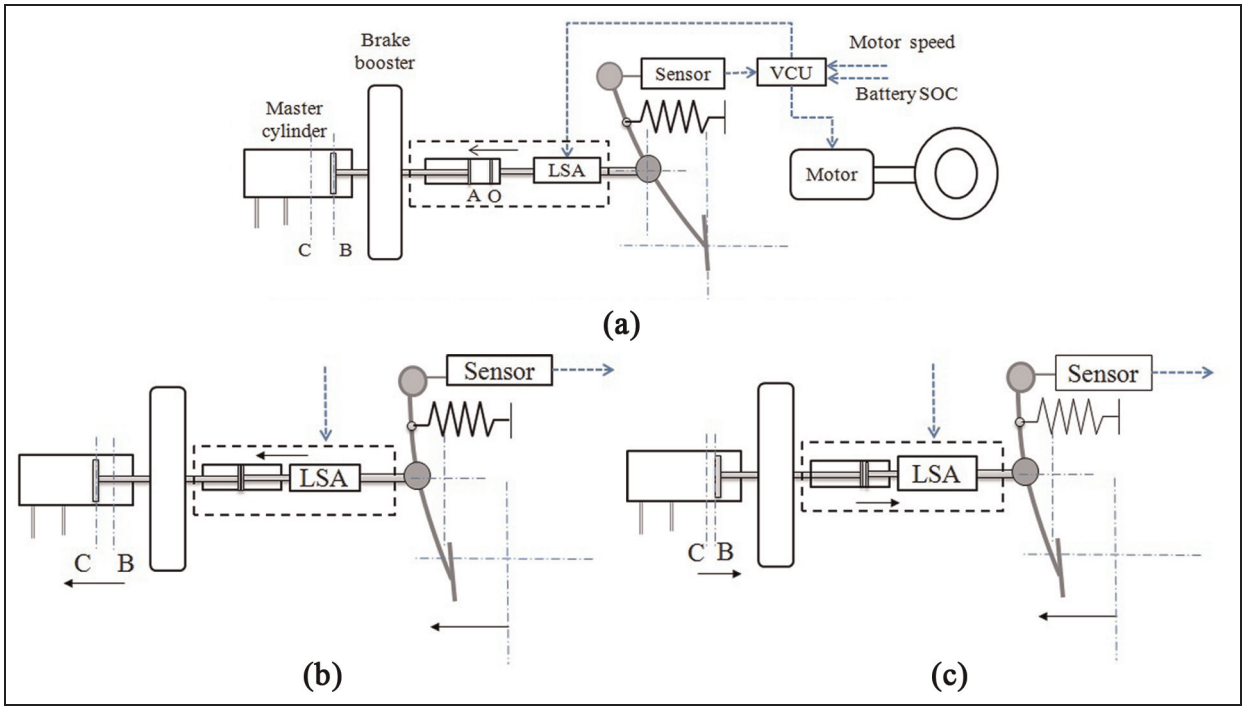

Figure 4. (a) Schematic layout of combined braking; (b) brake application beyond idle pedal travel; (c) braking in process at constant deceleration.
LSA: linear solenoid accelerator; VCU: vehicle control unit; SOC: state of charge.

Functionality and modelling. The function and the corresponding mathematical model of the proposed combined braking concept are explained below in the following three stages of the braking process. The braking process starts with depression of the brake pedal by the driver. Stage 1 corresponds to the phase where the brake pedal was moved from its initial position (zero displacement) to a final position as desired by the driver. Stage 2 and stage 3 correspond to the events that occur where the brake pedal is held at this desired final position by the driver.

Stage 1: brake application and determination of the idle actuator displacement OA. Before the brake application, the controller sets the value of OA by retracting the actuator plunger. In general, the value of OA is a function of the vehicle speed, the motor's braking power and the battery's SOC. In this study, the battery's SOC was assumed to be low to store the regenerated energy, and regenerative braking is applied only in the constant-power region of the electric motor. Let V_i be the initial vehicle speed at the instant of brake application. The idle actuator displacement OA was estimated on the basis of the regenerative braking force F_{reg} that the electric motor can generate with reference to the initial vehicle speed V_i and is given by

$$F_{reg} = \frac{P_m}{V_i} \tag{5}$$

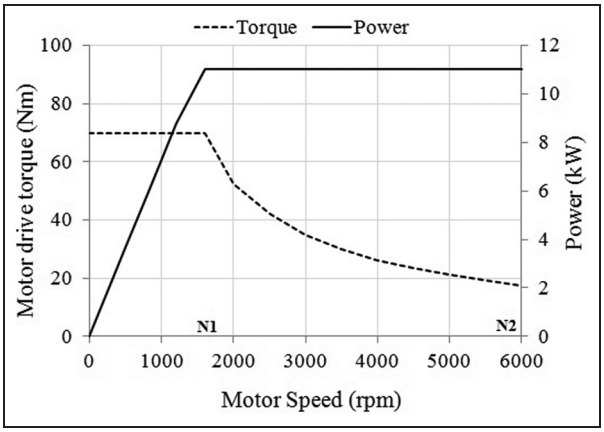

Figure 5. Characteristics of the motor used in the test vehicle.
rpm: r/min.

where P_m is the constant braking power of the motor. By substituting the value of F_{reg} in equation (4), the idle pedal displacement L_i was obtained as

$$L_i = B_0 F_{reg}^2 + B_1 F_{reg} + B_2 \tag{6}$$

The idle actuator displacement OA equivalent to L_i is given by

$$\mathrm{OA} = \frac{L_i}{\mathrm{PR}} \tag{7}$$

where PR is the pedal ratio.

Further, in this stage, braking can occur in two conditions as discussed in the following.

- *Condition 1: pedal displacement $L_p \leqslant$ idle pedal displacement L_i.* In this condition, only the regenerative brake is applied and the master cylinder is not actuated (thus, the friction brake is not applied).
- *Condition 2: pedal displacement $L_p >$ idle pedal displacement L_i.* In this condition, the LSA comes into contact with the brake booster's plunger and actuates the master cylinder (Figure 4(b)), and both the regenerative brake and the friction brake are applied. The master cylinder plunger is displaced by BC equivalent to the pedal displacement L_m.

Thus, the displacement BC of the master cylinder plunger can be written as

$$\mathrm{BC} = \begin{cases} 0 & \text{if} \quad L_p \leqslant L_i \\ \frac{L_p - L_i}{\mathrm{PR}} & \text{if} \quad L_p > L_i \end{cases} \tag{8}$$

Stage 2: braking in process and determination of the displacement BC of the master cylinder plunger. The schematic diagram of the combined braking layout corresponding to this stage is given in Figure 4(c).

The characteristics of the a.c. induction motor obtained from its product specification sheet[15] are shown in Figure 5. Since the motor power remains constant in the speed region between N_1 and N_2, regenerative braking is applied only when the vehicle speed corresponds to a motor speed in this region. At a motor speed less than N_1, only the friction brake is applied. The values of N_1 and N_2 are given in Table 1.

Since the braking power P_m of the motor is constant in the region of focus, the value of F_{reg} is higher at lower vehicle speeds. In the constant-power operating region, the regenerative braking force that the electric motor can generate at any instant of time t can be written as

$$F_{reg}(t) = \frac{P_m}{V(t)} \tag{9}$$

Hence, the frictional force required at that instant can be written as

$$F_{friction}(t) = F_b - F_{reg}(t) \tag{10}$$

where F_b is the total braking force to be generated by the system for the given brake pedal displacement L_p.

Hence, while braking is in process and the vehicle speed starts to decrease, there is a potential to increase the regenerative brake effort. This is realized by retracting the actuator plunger further inwards (Figure 4(c)), which reduces the displacement BC of the master cylinder plunger and hence the friction braking force, for the same pedal displacement L_p. The value of BC over the period of the braking time was calculated as follows. Using equation (4), the pedal displacement L_m equivalent to the frictional force demand $F_{friction}(t)$ at time t was obtained as

$$L_m(t) = A_0 \left[F_{friction}(t)\right]^2 + A_1 F_{friction}(t) + A_2 \tag{11}$$

Then, the corresponding displacement BC of the master cylinder plunger can be obtained using

$$\mathrm{BC}(t) = \frac{L_m(t)}{\mathrm{PR}} \tag{12}$$

At the same time, the motor current $I(t)$ is increased by the vehicle controller to meet the total braking force demand, which can be written as

$$I(t) = \frac{F_{reg}(t)\, V(t)}{U} \tag{13}$$

where U is the voltage. Using equations (9) to (13), the displacement BC of the master cylinder plunger was calculated while braking.

Stage 3: vehicle speed below the threshold. At a motor speed less than N_1, the voltage output from the motor is reduced to less than the battery voltage and hence the battery cannot be charged. Hence, the regenerative brake is not applied when the vehicle speed is lower than the corresponding threshold vehicle velocity V_{th}, which can be obtained using

$$V_{th} = \frac{1 - S}{\mathrm{TR}} \frac{2\pi N_1}{60}\, r \tag{14}$$

In this stage, only the friction brake is applied and the regenerative brake is set to zero; consequently, the idle pedal travel OA is zero. This is realized by energizing the solenoid actuator to actuate the master cylinder plunger directly.

The flow chart describing the combined braking process is shown in Figure 6.

Conventional parallel braking

In existing conventional parallel braking, both the friction brake and the regenerative brake are applied simultaneously. The electric motor directly applies its braking torque to the driven wheels (the rear wheels) and is controlled by the vehicle controller, based on the vehicle speed and the brake pedal displacement, which represents the brake demand. The friction brake is applied on both driven wheels and non-driven wheels based on the brake pedal displacement irrespective of the braking force generated from the electric motor. This type of configuration is common in EVs or HEVs which have a mechanically controlled friction brake. Sharing of the braking force between the regenerative brake and the friction brake in parallel braking is shown in Figure 7. As shown in the figure, up to a pedal displacement point Q, the regenerative brake is gradually increased, beyond which it remains constant. This point Q depends on the braking power of the

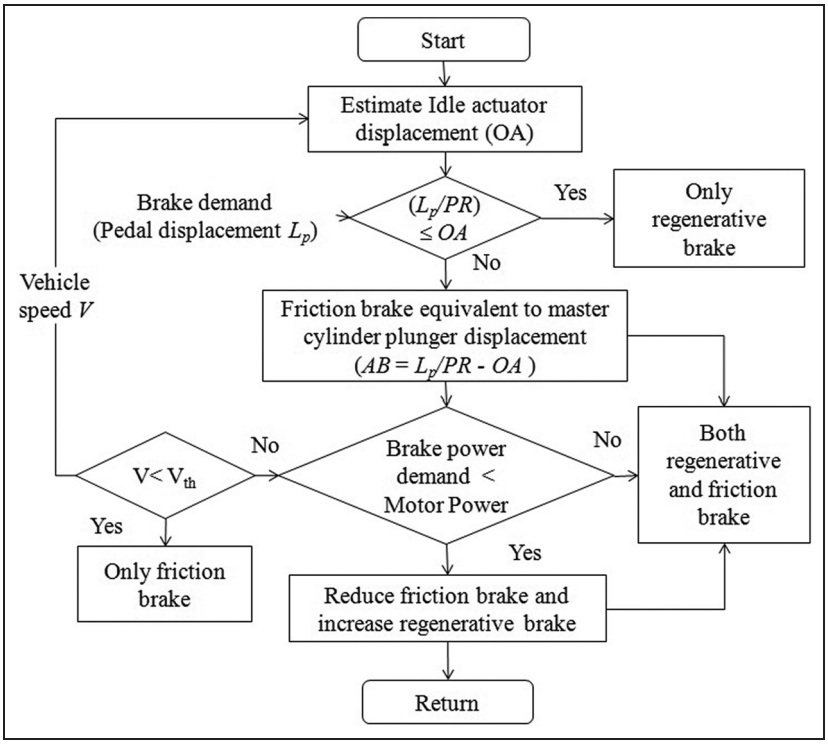

Figure 6. Flow chart for combined braking.

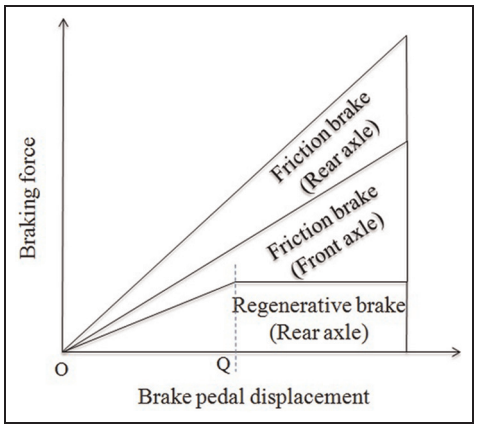

Figure 7. Sharing of the braking force in parallel braking.

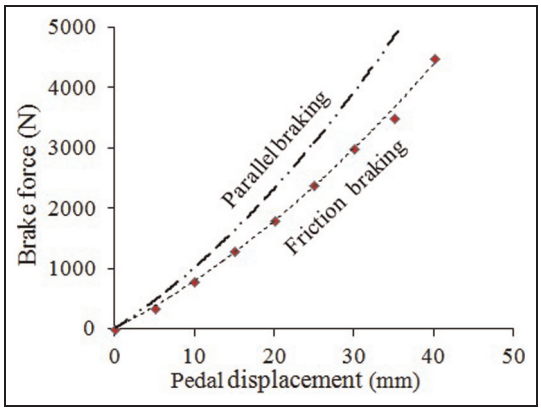

Figure 8. Characteristics of conventional parallel braking.

motor and the braking power demand of the vehicle. Since the braking force is always shared between the friction brake and the regenerative brake, the potential for energy regeneration is less in conventional parallel braking.

The regenerative braking force F_{reg} generated in conventional parallel braking is a fixed proportion γ of the total brake demand, which can be written as

$$F_{reg} = \begin{cases} \gamma F_b & \text{if} \quad \gamma F_b < \frac{P_m}{V} \\ \frac{P_m}{V} & \text{if} \quad \gamma F_b > \frac{P_m}{V} \end{cases} \tag{15}$$

where F_b is the braking force demand, calculated from equation (3), for a given brake pedal displacement L_p. The total braking force generated in conventional parallel braking is the sum of the regenerative braking force and the frictional braking force, which is given by

$$F_{b(Parallel)} = F_b + F_{reg} \tag{16}$$

When the vehicle speed is below the threshold value V_{th} (corresponding to a motor speed less than N_1), the vehicle controller sets the regenerative braking force to zero. In conventional parallel braking, since the regenerative brake was applied in addition to the friction brake, the system characteristics were modified as shown in Figure 8. However, during certain conditions such as a high SOC of the battery or a vehicle speed below the threshold value, the regenerative braking force is set to zero and only the friction brake will be activated. This demands additional pedal displacement

to meet the conventional parallel braking characteristics. This additional pedal displacement is a function of γ; the higher the γ value, the higher is the additional pedal displacement, which affects the driveability of the vehicle.[10] In this study, the value of γ was selected as 0.3, with the objective that the additional pedal displacement when the regenerative braking force is zero does not exceed 7 mm.

Braking force distribution

The BFD between the front wheels and the rear wheels should balance the dynamic forces of the vehicle for the optimum braking performance and stable braking.[12] Since regenerative braking is applied on only the drive (rear) wheels in the vehicle considered, an analysis was performed to understand the BFD for different regenerative braking strategies.

The BFD between the front wheels and the rear wheels is limited by various curves such as the I curve, the β line, the F line and the R line.[14] The I curve is the theoretical non-linear curve plotted between F_{bf}/Mg and F_{br}/Mg for various road adhesion coefficients μ and deceleration levels a/g. This curve characterizes the ideal BFD between the front wheels and the rear wheels, considering the dynamic loads acting on each wheel.

The variables F_{bf} and F_{br} are the maximum braking force that can be applied on the front wheels and the maximum braking force that can be applied on the rear wheels respectively without wheel lock and are limited by the road adhesion coefficients and the dynamic loads acting on the wheels; they are given by

$$\begin{aligned} F_{bf} &= \mu\, W_{f(dynamic)} \\ F_{br} &= \mu\, W_{r(dynamic)} \end{aligned} \tag{17}$$

where $W_{f(dynamic)}$ and $W_{r(dynamic)}$ are the dynamic load acting on the front wheels and the dynamic load acting on the rear wheels respectively.

The dynamic load acting on the front wheels and the dynamic load acting on the rear wheels can be written as (Figure 9)

$$\begin{aligned} W_{f(dynamic)} &= \frac{Mg}{L}\left(L_b + h\frac{a}{g}\right) - F_a\frac{h}{L} \\ W_{r(dynamic)} &= \frac{Mg}{L}\left(L_b - h\frac{a}{g}\right) + F_a\frac{h}{L} \end{aligned} \tag{18}$$

where g is the acceleration due to gravity, L is the wheelbase, L_a and L_b are the distance of the front axle from the centre of gravity and the distance of the rear axle from the centre of gravity respectively and h is the height of centre of gravity from the ground.

The actual braking forces applied on the front wheels and on the rear wheels by the brake system are usually designed to have fixed linear proportions, giving the design parameter[3] β which is defined as follows: β is the ratio of the braking force on the front wheels

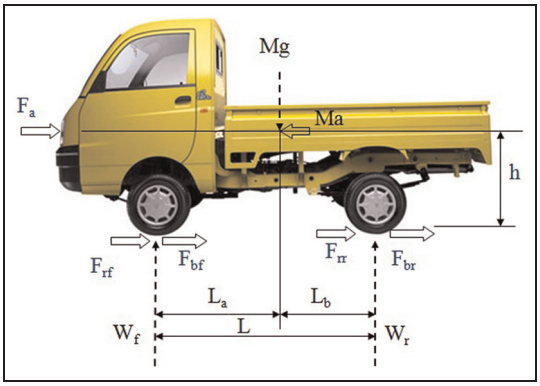

Figure 9. Longitudinal forces while braking.

to the total braking force acting on the vehicle, which can be written as

$$\beta = \frac{F_{bf}}{F_b} \tag{19}$$

The braking force on the front wheels and the braking force on the rear wheels generated by the brake system can be written as

$$F_{bf} = \beta F_b$$

and

$$F_{br} = (1-\beta)F_b$$

respectively. Thus, the ratio of the braking force generated by the brake system on the front wheels to the braking force generated by the brake system on the rear wheels can be written as

$$\frac{F_{bf}}{F_{br}} = \frac{\beta}{1-\beta} \tag{20}$$

The value of β was estimated from the vehicle parameters and the longitudinal dynamic response as discussed below. In this study, the value of β was fixed on the basis of the requirement that, on a dry asphalt flat road with an adhesion coefficient $\mu_0 = 0.8$, both the front wheels and the rear wheels lock at the same time. In other words, it can be said that the I curve and the β line intersect at $a/g = \mu_0 = 0.8$. Based on this requirement, the corresponding value of β is obtained by replacing a/g in equation (14) with μ_0, which can be written as

$$\begin{aligned} \frac{F_{bf}}{F_{br}} &= \frac{\beta}{1-\beta} \\ &= \frac{(Mg/L)(L_b + h\mu_0) - F_a(h/L)}{(Mg/L)(L_a - h\mu_0) + F_a(h/L)} \end{aligned}$$

From the above equation, β can be written as

$$\beta = \frac{(Mg/L)(L_b + h\mu_0) - F_a(h/L)}{Mg} \tag{21}$$

Table 3. Experimental vehicle drive specifications.

Maximum speed	45 km/h
Gradeability	16°
Acceleration speed	0–40 km/h
Acceleration time	20 s
Acceleration	0.56 m/s^2

By substituting $\mu_0 = 0.8$ and the vehicle parameter values given in Table 1, the value of β was calculated as 0.6. In a rear-wheel-drive HEV, the regenerative brake acts on the rear wheels, and the friction brake acts on both the front wheels and the rear wheels. Therefore, the braking force on the front wheels and the braking force on the rear wheels can be written as

$$F_{bf} = \beta F_{friction} \tag{22}$$

and

$$F_{br} = (1 - \beta)F_{friction} + F_{reg} \tag{23}$$

respectively. For different road adhesion coefficients μ, the equations governing the F line and the R line can be written as[14]

$$F_{br} = \frac{L - \mu h}{\mu h} F_{bf} - \frac{MgL_b}{h} \tag{24}$$

$$F_{br} = \frac{-\mu h}{L + \mu h} F_{bf} + \frac{\mu MgL_a}{L + \mu h} \tag{25}$$

Equations (17) to (25) were used in plotting the BFD limiting curves.

Simulations

To evaluate the proposed combined braking concept and to compare the energy regeneration and the BFD with those of conventional parallel braking, simulations were performed using the experimental vehicle parameters given in Table 1 and the drive specifications given in Table 3. The simulations were carried out in city braking conditions, highway braking conditions and across the Modified Indian Driving Cycle (M-IDC).

Normal (city and highway) braking

As measured by Shah et al.,[13] the average driving speed on Indian highways is about 90 km/h and the average driving speed in Indian cities is about 40 km/h. These average speeds were considered as the initial vehicle speed in the normal braking simulations. The other parameters considered in the simulations are given in Table 4.

The threshold vehicle speed V_{th} given in Table 4 was estimated using equation (1) and the vehicle data given in Table 1. The average braking power demand P_b was calculated from the total braking force demand F_b and the average vehicle speed V_a, which can be written as

$$P_b = F_b V_a$$

Table 4. Normal deceleration braking conditions.

	Value for the following	
	Highway	City
Initial vehicle speed V_i (km/h)	90	40
Threshold vehicle speed V_{th} (km/h)	10	10
Braking time t (s)	12	10
Braking deceleration a (units of g)	0.21	0.11
Average braking power P_b (kW)	37.8	9.8
Fixed ratio γ	0.2	0.2
Fixed ratio β	0.6	0.6

Table 5. Pedal displacement at different braking conditions.

	Value for the following	
	Highway	City
Idle actuator displacement OA (mm)	0.8	1.80
Total actuator displacement L_p/PR (mm)	5.83	3.33
OA as a percentage of L_p/PR	13%	54%

PR: brake pedal ratio.

Table 6. Values of energy regenerated under different conditions.

	Energy regenerated (W h)	
	Highway	City
Conventional parallel braking	23	7
Combined braking	27	18
Improvement	17%	157%

The idle and total actuator displacements were estimated using equations (5) to (7) for both highway braking conditions and city braking conditions, and the values are given in Table 5.

The energy regenerated in the braking process was calculated using

$$E_{reg} = \int_{t_0}^{t_1} F_{reg}(t)V(t)\,\mathrm{d}t \tag{26}$$

The regenerative energy was calculated for different braking scenarios, and the results are presented in Table 6.

As given in Table 5, the improvement in energy regeneration was high during city braking. This shows that the proposed combined braking strategy is more effective when the motor power is equivalent to or greater than the brake power demand. When the motor

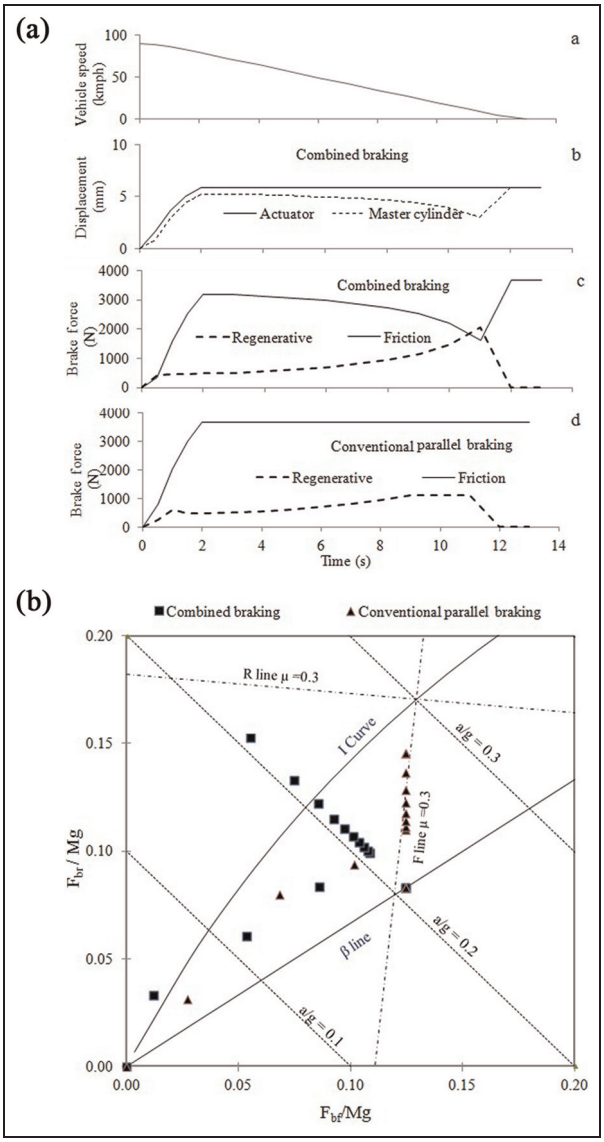

Figure 10. Highway braking scenario: (a) sharing of the braking force; (b) BFD.
kmph: km/h.

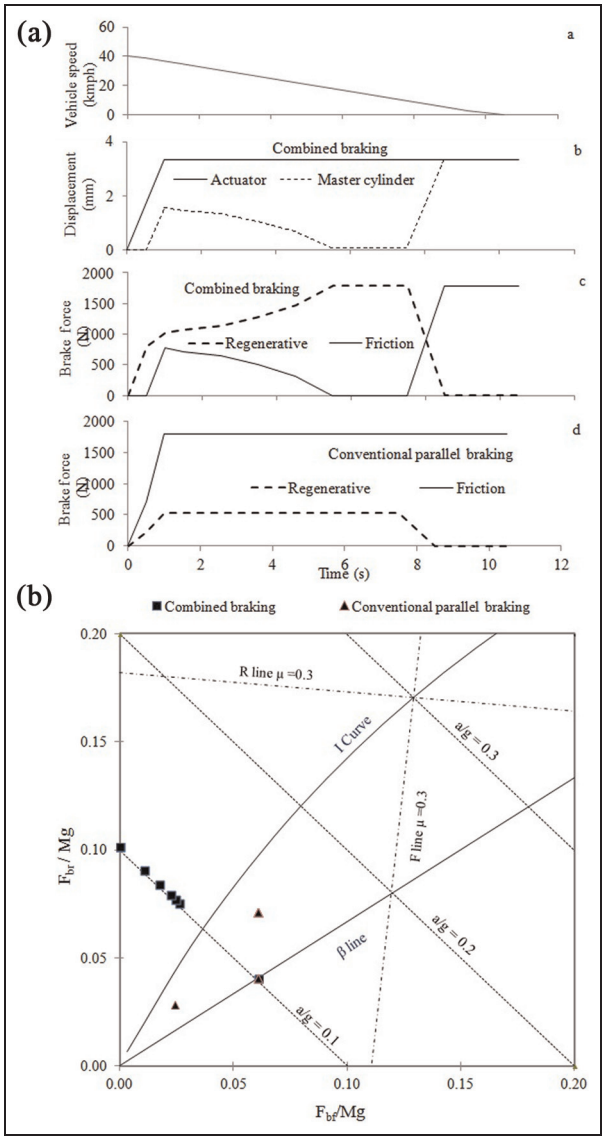

Figure 11. City braking scenario: (a) sharing of the braking force; (b) BFD.
kmph: km/h.

power is less than the brake power demand, the improvement in energy regeneration is not so significant.

The simulation plots for different braking scenarios are shown in Figure 10(a) and Figure 11(a), in which the subplot a shows the vehicle speed over time and the subplot b shows the displacement BC of the master cylinder plunger and the actuator displacement L_p/PR. The subplot c and the subplot d show the sharing of the braking force between the friction brake and the regenerative brake over time in combined braking and conventional parallel braking respectively.

From these subplots a to d in both Figure 10(a) and Figure 11(a), the following observations were made.

1. The displacement of the master cylinder plunger (subplot b) is reduced with decreasing vehicle speed (subplot a).
2. The level of friction braking decreases (subplot c) corresponding to a decrease in the displacement of the master cylinder plunger (subplot b).
3. In combined braking (subplot c), the decrease in the friction braking force is balanced by the regenerative braking force.

In conventional parallel braking, the amount of regenerative braking is lower (subplot d) than in combined braking (subplot c).

Figure 10(b) and Figure 11(b) show the BFD plots in highway braking and city braking respectively. From these figures, the following observations were made.

1. As shown in Figure 10(b) (highway braking), at a maximum deceleration of 0.2g, the BFD is closer to the β line in conventional parallel braking, whereas it is closer to the I curve in combined

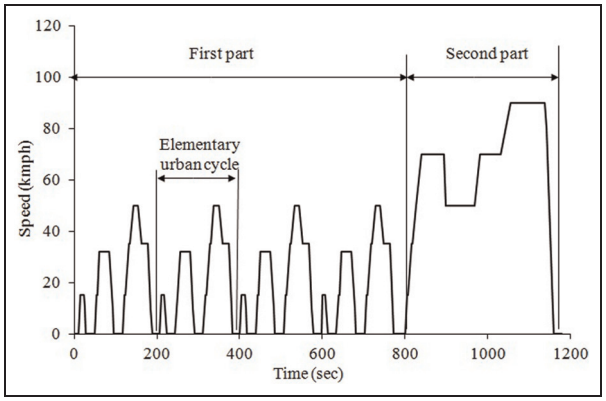

Figure 12. M-IDC.
kmph: km/h.

braking. As explained in the previous section, the I curve represents the braking force on the front wheels and the rear wheels that meets the corresponding dynamic limits of the vehicle.

2. Thus, the combined braking strategy is able to utilize the tyre–road traction better than conventional parallel braking, leading to more stable braking and a stable dynamic response of the vehicle.
3. In Figure 11(b) (city braking), the combined BFD points are closer to the vertical axis, which shows that the total braking force is generated by the motor (at the rear wheels) in most cases. Thus, when the motor braking power is equivalent to the braking power required, the BFD points move towards the vertical axis. It can be observed that all the BFD points lie within the F line and the R line (corresponding to $\mu = 0.3$) and, hence, the vehicle is stable even on road surfaces with $\mu = 0.3$, with the combined braking strategy.

Driving cycle

The energy regenerated by the vehicle (the parameters of which are given in Table 1) across the M-IDC where both a conventional parallel braking strategy and a combined braking strategy were simulated. The M-IDC, as shown in Figure 12, was developed by the Automotive Research Association of India;[16] it is a synthesized driving cycle simulated in a chassis dynamometer on a test vehicle and contains two parts. The first part contains four elementary urban driving cycles and the second part contains an extra urban cycle. The maximum speed, the maximum acceleration and the maximum deceleration are 50 km/h, 1.04 m/s^2 and 0.99 m/s^2 respectively in the first part and 90 km/h, 0.83 m/s^2 and 1.39m/s^2 respectively in the second part.

The total braking energy recoverable from the vehicle across the driving cycle was estimated using

$$E_{rec} = \int_{t_0}^{t_1} \delta M \frac{\Delta V}{\Delta t} V \, dt - \int_{t_0}^{t_1} M g f_r V \, dt - \int_{t_0}^{t_1} \frac{\rho C_d A_f V^2}{2} V \, dt \quad (27)$$

Table 7. Values of energy regenerated across the M-IDC.

	Energy (W h)
Conventional parallel braking	103
Combined braking	213
Improvement	106%

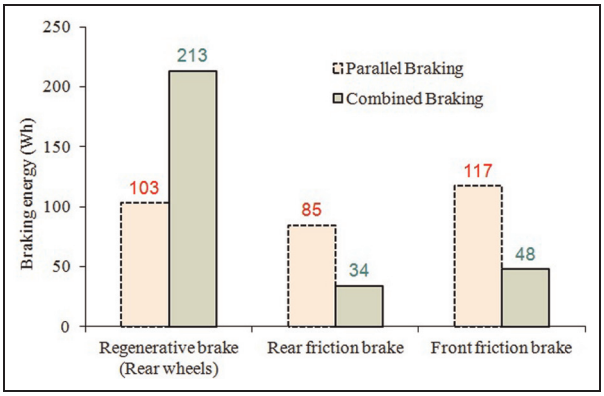

Figure 13. Braking energy across the M-IDC.

Using equation (27) and the equations presented in the third section, the total energy regenerated was obtained, and the results are given in Table 7. It can be observed that the energy regeneration with the proposed combined braking strategy is almost twice that with conventional parallel braking.

Figure 13 shows the braking energy shared between the friction brakes at the front wheels and the rear wheels and the regenerative brake at the rear wheels. Conventional parallel braking regenerates only 34% of the total braking energy whereas combined braking regenerates 72% of the total braking energy.

The BFD points for both the conventional parallel braking strategy and the combined strategy across the M-IDC were calculated and plotted in Figure 14. The BFD points for combined braking are in between the I curve and the vertical axis, which indicates that the rear wheels have a larger share of the braking force.

Road testing

The experimental vehicle (Figure 15) used in the road test was a rear-wheel-drive light commercial vehicle[17] which is converted into an SHEV. The system layout of the experiment vehicle (shown in Figure 1) consist of an a.c. induction motor with a power rating of 11 kW coupled with a single-stage gearbox, with a gear ratio of 2.9. A 0.9 l engine connected to a 24 kW generator was used to charge the battery pack. 16 units of 6 V lead–acid batteries were connected in series to create a potential difference of 96 V with an energy capacity of 24 kW h. An onboard battery charger was used to charge the 96 V battery back from the grid. Both the motor

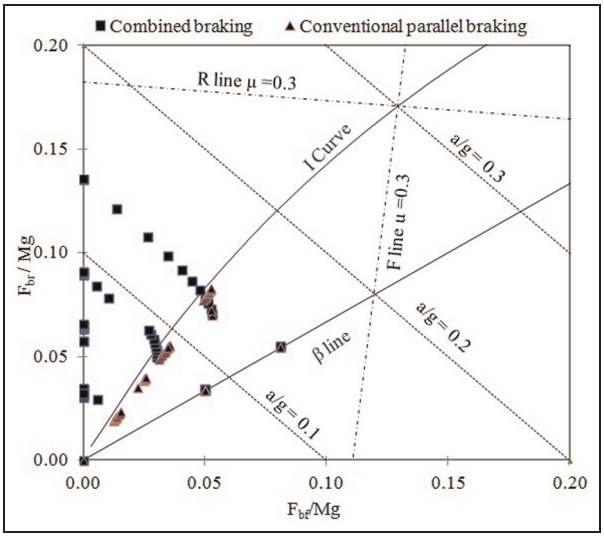

Figure 14. BFD points across the M-IDC.

Figure 15. Experimental vehicle.

controller and the generator controller operate in the voltage range 72–96 V. The other parameters of the vehicle are listed in Table 1.

The inputs and the output signals such as the speed, the current and the voltage of the motor and the battery SOC and the voltage of the battery were transferred through the controller area network (CAN). The regenerative motor torque command for the regenerative brake was carried out by the CAN with the vehicle controller and the motor controller. The brake pedal displacement was measured with a linear position sensor, and the data were collected from a data acquisition system. From information on the current and the voltage of the motor, the energy regenerated while braking was calculated using

$$E = \int_{t_0}^{t_1} UI \, \mathrm{d}t \tag{28}$$

The normal braking test and a driving-cycle test were conducted in the experimental vehicle with both the parallel braking strategy and the combined braking strategy.

Table 8. Values of energy regenerated in different braking conditions.

	Energy regenerated (W h)	
	Simulations	Experiments
Conventional parallel braking	7	8.3
Combined braking	18	18.5
Improvement	157%	122%

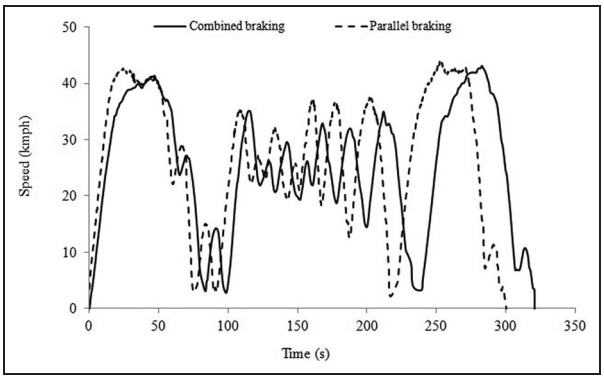

Figure 16. Experimental speed plots.
kmph: km/h.

Normal braking test

As mentioned in Table 3, since the maximum speed of the experimental vehicle is 45 km/h, the normal braking test was carried out only in city driving conditions, with an initial speed of 40 km/h until zero speed on a flat dry asphalt road. Both the conventional parallel strategy and the combined braking strategy were applied to measure the energy regeneration. The brake pedal displacement L_p was maintained at a constant value, corresponding to a deceleration demand of 0.11g. From the measured current and voltage data of the motor, the values of the energy regenerated were estimated using equation (28) and are given in Table 8. The measured data were compared with the corresponding simulation results (given in Table 6), where the initial speed and the deceleration demand were the same as in the experiments. It can be observed that the values predicted by the simulations agree well with those from the experiments, particularly for combined braking.

Driving-cycle test

Since it is difficult to reproduce the M-IDC (shown in Figure12) on the road, the vehicle was tested on a real time speed–time plot, which is shown in Figure 16. The test vehicle was operated on almost the same speed–time plot for both combined braking and conventional parallel braking. With the measured current and voltage values of the battery, the energy regenerated was estimated using equation (28), and the results are given

Table 9. Values of energy regenerated in real time–speed plots.

	Energy regenerated (Wh)	
	Simulations	Experiments
Conventional parallel braking	34	38
Combined braking	85	79
Improvement	150%	107%

in Table 8. With this experimental speed–time plot (Figure 16), simulations were repeated to measure the energy regeneration. Both the simulated values and the experimental values are given in Table 9.

From the above experimental results, the following conclusions are drawn.

1. In both normal city braking and the real-time driving-cycle test, the combined braking regenerates almost twice the energy regenerated by conventional parallel braking.
2. Also, the simulations and the experimental results agree well, and this corroborates the mathematical approach followed.

Conclusions

From the simulation results and the vehicle testing, the following conclusions were drawn on the proposed combined braking.

1. With a motor power equivalent to or more than the vehicle braking power demand, the proposed combined braking strategy can regenerate more than twice the energy that conventional parallel braking does.
2. The BFD was improved in combined braking, which leads to a stable vehicle response during braking.

The novelty features of this paper are the proposal and analysis of an innovative concept for improving the regenerative braking energy in EVs and HEVs which are equipped with a mechanical friction brake system. This concept will hopefully aid the development and acceptance of EVs and HEVs in the emerging markets by improving their operating economy.

A summary of this paper is as follows.

1. A detailed study was made and a new regenerative braking concept called combined braking was presented for an SHEV which has a mechanically controlled friction brake.
2. The energy regenerated with combined braking is found to be double that with conventional parallel braking in an urban driving scenario. This was simulated and corroborated in vehicle testing, which is significant for improving the fuel efficiency of a vehicle in city driving.
3. The BFD was analysed for combined braking and it was found that it was able to utilize the tyre–road traction better than that for conventional parallel braking, leading to more stable braking and a stable dynamic response of the vehicle.

The proposed approach is a starting point for deployment in EVs and HEVs which have only a mechanically controlled friction braking system. The integration of this system with safety mechanisms such as anti-lock brake systems and its overall effect on vehicle dynamics are the tasks that are being carried out in the continuing phase of the research presented.

Declaration of conflict of interest

The authors declare that there is no conflict of interest.

Funding

This research received no specific grant from any funding agency in the public, commercial or not-for-profit sectors.

References

1. Ahn J, Jung K, Kim D et al. Analysis of a regenerative braking system for hybrid electric vehicles using an electro-mechanical brake. *Int J Automot Technol* 2009; 10(2): 229–234.
2. Li Y-S, Zeng Q-L, Wang C-L and Wang L. Research on control strategy for regenerative braking of a plug-in hybrid electric city public bus. In: *2nd IEEE international conference on intelligent computation technology and automation*, Changsha, Hunan, People's Republic of China, 10–11 October 2009, Vol 1, pp. 842–845. New York: IEEE.
3. Muta K, Yamazaki M and Tokieda J. Development of new-generation hybrid system TSH II – drastic improvement of power performance and fuel economy. SAE paper 2004-01-0064, 2004.
4. Yeo H and Kim H. Hardware-in-the-loop simulation of regenerative braking for a hybrid electric vehicle. *Proc IMechE Part D: J Automobile Engineering* 2002; 216(11): 855–864.
5. Jo C, Ko J, Yeo T et al. Cooperative regenerative braking control algorithm for an automatic-transmission-based hybrid electric vehicle during a downshift. *Proc IMechE Part D: J Automobile Engineering* 2012; 226(4): 457–466.
6. Aoki Y, Suzuki K, Nakano H et al. Development of hydraulic servo brake system for cooperative control with regenerative brake. SAE paper 2007-01-0868, 2007.
7. Zhang J, Chen X and Zhang P. Integrated control of braking energy regeneration and pneumatic anti-lock braking. *Proc IMechE Part D: J Automobile Engineering* 2010; 224(5): 587–610.
8. Albrichsfeld C and Karner J. Brake system for hybrid and electric vehicles. SAE paper 2009-01-1217, 2009.

9. Zhang J, Lv C, Gou J and Kong D. Cooperative control of regenerative braking and hydraulic braking of an electrified passenger car. *Proc IMechE Part D: J Automobile Engineering* 2012; 226(10): 1289–1302.
10. Zhang J, Lu X, Xue J and Li B. Regenerative braking system for series hybrid electric city bus. *World Electric Veh J* 2008; 2(4): 128–134.
11. Hancock M. Impact of regenerative braking on vehicle stability. In: *Institution of Engineering and Technology hybrid vehicle conference*, Coventry, Warwickshire, UK, 12–13 December 2006, pp. 173–184. Stevenage, Hertfordshire: Institution of Engineering and Technology
12. Beiker S and Vachenauer R. The impact of hybrid-electric powertrains on chassis system and vehicle dynamics. SAE paper 2009-01-0442, 2009.
13. Shah V, Patel P, Patel S et al. Measurement of real time drive cycle for Indian roads and estimation of component sizing for HEV using LABVIEW. *World Acad Sci, Engng Technol* 2011; 5(10): 648–656.
14. Ehsani M, Gao Y and Emadi A. *Modern electric, hybrid electric and fuel cell vehicles – fundamentals, theory and design*. Boca Raton, Florida: CRC Press, 2010.
15. HPEVS, Hi Performance Electric Vehicle Systems. Links to power graphs, http://hpevs.com/power%20graphs.htm (2012–2015, accessed August 2013).
16. Type I test on SI, engines, CNG, LGP and diesel engined vehicles (verifying the average tailpipe emission of gaseous and particulate pollutants). CMVR type approval document MoRTH/CMVR/TAP-115-116, Part 09, ch 03, pp. 313–343, Automotive Research Association of India, Pune, India 2000, https://www.araiindia.com/CMVR_TAP_Documents/Part-11/Part-11_Chapter 03.pdf (2000, accessed January 2012).
17. Mahindra Maxximo Plus. Technical specification, http://www.mahindramaxximoplus.com/net/specification.html (2013, accessed June 2013).

Appendix 1

Notation

a	acceleration or deceleration in the longitudinal direction
A_f	frontal cross-sectional area
C_d	coefficient of drag
E	energy
f_r	rolling resistance coefficient of the tyres
F_a	aerodynamic force
F_b	total braking force
F_{bf}	braking force at the front axle
F_{br}	braking force at the rear axle
F_{reg}	regenerative force
g	acceleration due to gravity
h	height of the centre of gravity from the ground
I	current of the motor
M	mass of the vehicle
N	speed of the motor
N_1	base speed of the motor
N_2	maximum speed of the motor
L	wheelbase
L_a	distance from the centre of gravity to the front axle
L_b	distance from the centre of gravity to the rear axle
L_i	idle pedal displacement
L_p	brake pedal displacement
PR	brake pedal ratio
P_m	braking power of the motor
r	effective radius of the tyres
S	tyre slip
TR	transmission ratio
t	braking time
U	voltage of the battery
$W_{f(dynamic)}$	dynamic load of the front axle
$W_{r(dynamic)}$	dynamic load of the rear axle
V	speed of the vehicle
β	ratio of the braking force on the front wheels to the total braking force on the vehicle
γ	ratio of the regenerative force to the total braking force
μ	coefficient of friction between the road and the tyres
ρ_a	density of air